GEOPHYSICAL RESEARCH LETTERS, VOL. 20, NO. 20, PAGES 2259-2262, OCTOBER 22, 1993

ULYSSES OBSERVATIONS OF AURORAL HISS AT HIGH JOVIAN LATITUDES

W. M. Farrell[1], R. J. MacDowall[1], M. D. Desch[1], M. L. Kaiser[1], R. G. Stone[1], P. J. Kellogg[2], N. Lin[2], N. Cornilleau-Wehrlin[3], P. Canu[3], S. J. Bame[4], and J. L. Phillips[4]

Abstract. During the Ulysses flyby of Jupiter, a whistler-mode emission was periodically detected by the Unified Radio and Plasma wave (URAP) experiment during intervals when the spacecraft extended to high magnetic latitudes. The signal was detected between the local electron plasma frequency and lower hybrid resonance and appears as a funnel-shaped structure on frequency-versus-time spectrograms; these characteristics are very reminiscent of whistler-mode auroral hiss observed at high latitudes at Earth. Ray tracing of the emission occurrences suggests the emission source is on magnetic field lines extending out to at least 65 R_J. This location associates the emission with the boundary between open and closed field lines — not the Io torus. The emission radiates about 10^7 W of power. Consequently, the auroral input power derived from the solar wind to drive the emission is believed to be 10^{10-12} W (or about 1% of the energy associated with Io torus electrical processes).

Introduction

In February of 1992, the Ulysses probe flew by the planet Jupiter to swing the spacecraft into an inclined solar orbit extending to high heliospheric latitudes ($\sim 80°$). Although the primary purpose of the encounter was navigational, it gave Ulysses science investigators an opportunity to study the dynamics of the Jovian magnetosphere. For example, as the spacecraft reached high magnetic latitudes near closest approach, a whistler-mode emission was observed extending in frequency from near the electron plasma frequency down to approximately the lower hybrid frequency [Stone et al., 1992b]. On a radio spectrogram, the emission appeared funnel-shaped and is very similar to auroral hiss observed in the terrestrial polar cusp [Gurnett and Frank, 1978] and nightside auroral regions [Gurnett et al., 1983]. The characteristics of this emission, which is the Jovian analog to terrestrial auroral hiss emission (i.e., Jovian auroral hiss), will be discussed in this paper.

The Ulysses URAP experiment consists of five separate instruments: the radio astronomy receiver (RAR) with 76 channels between 1.25 and 940 kHz, the plasma frequency receiver (PFR) with 32 channels between 0.57 and 35 kHz, the fast envelope sampler (FES) which samples at 1 msec resolution in two broad passbands, the waveform analyzer (WFA) covering 0.08 to 448 Hz, and an active sounder. For further information on these instruments, see Stone et al., [1983, 1992a,b]. The observations presented here are derived from the WFA and PFR, with supporting electron measurements from the solar wind plasma experiment [Bame et al., 1992a]. The WFA samples both electric and magnetic (search coil) antennae. The new availability of AC magnetic information at Jupiter should not be understated, since the cB/E ratio and radiated power can be estimated for the wave components below 448 Hz.

Figure 1 is a color dynamic spectrum combining measurements from the Ulysses WFA and PFR receivers showing examples of the auroral hiss emission. Superimposed on the spectrogram is the electron cyclotron frequency, f_{ce}, electron plasma frequency, f_{pe}, and lower hybrid frequency, f_{LHR}, derived from the electron plasma measurements and the O4 magnetic field model [Connerney et al., 1981]. The plasma frequency was also verified in some instances by the URAP sounder operating between 1.2 kHz and 48.5 kHz. The lower hybrid frequency is defined for a single component proton plasma. During periods when the spacecraft extended to high latitudes, a funnel-shaped emission became apparent, residing between f_{pe} and f_{LHR}. Since the emission lies below the electron plasma frequency, it is identified as whistler-mode. The emission regularly reappeared each rotation as the spacecraft passed through high latitudes. In fact, three events near closest approach, those occurring around hour 1200 and 2200 of February 7 and 0600 February 8, are associated with Ulysses entering regions where solar wind-like particle signatures were observed [Bame et al., 1992b; Simpson et al., 1992].

Figure 2 displays the (a) electric and (b) magnetic spectral densities as a function of wave frequency during a high latitude excursion by Ulysses (1300 SCET). For reference, a later time without auroral hiss is shown. Like the spectrogram in Figure 1, enhanced wave frequencies are observed between about 20 Hz (i.e., near f_{LHR}) to about 500 Hz. The corresponding cB/E ratios of the auroral hiss ranges between 1–10, suggesting that the emission has a relatively strong magnetic component. Such cB/E values are consistent with those observed for terrestrial auroral hiss emissions generated by electron beams of moderate energies [Gurnett et al., 1986]. The enhanced activity in the electric field measurements below 10 Hz may be either real electrostatic turbulence or low frequency noise generated by the onboard modified Walsh transform.

At earth, auroral hiss was commonly observed from the polar cusp region by spacecraft like Hawkeye-1 and Dynamics Explorer-1 [Gurnett and Frank, 1978; Gurnett et al., 1983; Lin et al., 1984]. The emission has its distinct shape on a spectrogram because it propagates with wave normal vectors very near the resonance cone. Figure 3 shows the index of refraction as a function of wave normal angle, θ, (i.e., an index of refraction surface). At a limiting angle, known as the resonance cone angle, θ_{res}, the index of refraction

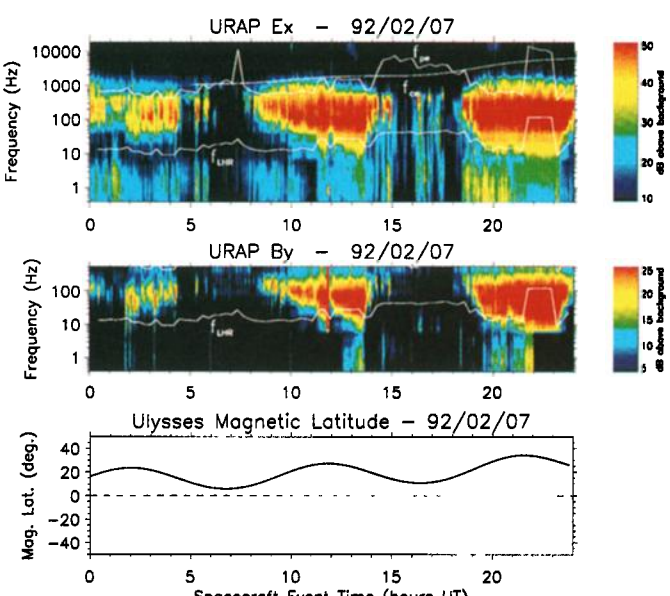

Fig 1. URAP (a) electric and (b) magnetic field measurements, along with (c) spacecraft magnetic latitude during a period when three auroral hiss events were observed. Note that the events were observed only during periods when Ulysses extended to relatively high magnetic latitudes.

1. NASA/Goddard Space Flight Center
2. Univ. of Minnesota, School of Astronomy & Astrophysics
3. Centre de Recherches en Physique de l'Environnement Terrestre et Planetaire (CRPE)
4. Space Plasma Physics Group, Los Alamos National Laboratory

Paper number 93GL01120
0094-8534/93/93GL-01120$03.00

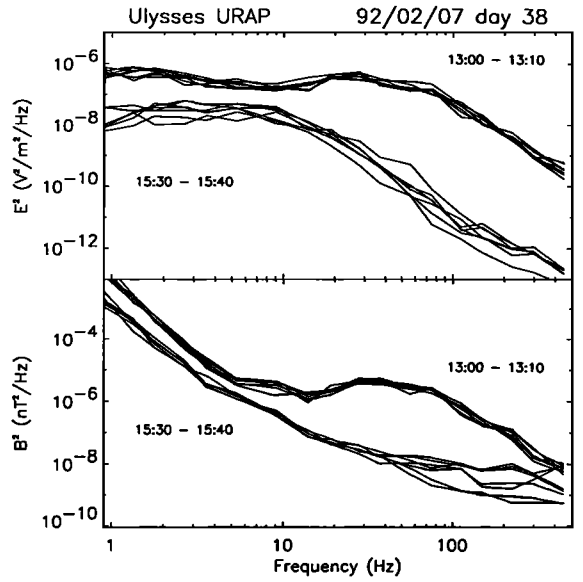

Fig 2. The (a) electric and (b) magnetic spectral densities during a period when the auroral hiss signals were observed by the WFA experiment.

goes to infinity. This angle is defined as $\mathrm{Tan}^2\,\theta_{res} = -\epsilon_{zz}/\epsilon_{xx}$ where $\epsilon_{zz} = 1 - f_{pe}^2/f^2$ and $\epsilon_{xx} = 1 - f_{pe}^2/(f^2 - f_{ce}^2)$ are elements of the cold plasma dielectric tensor (e.g., Gurnett [1983]) . The group velocity vector, v_g, is always normal to the index of refraction surface.

There are a number of interesting wave characteristics for propagation near the resonance cone angle. First, the wave becomes electrostatic, with the wave electric field becoming more parallel to the wave normal vector, k, as the normal angle approaches the resonance cone angle, θ_{res}. Second, for wave normal angles near the resonance cone angle, v_g is nearly perpendicular to the wave normal vector, k. Finally, the resonance cone angle decreases with increasing wave frequency. Consequently, v_g becomes more oblique to the ambient magnetic field with increasing frequency. Thus, high frequency emissions tend to be beamed at larger angles with respect to the local magnetic field than those at lower frequencies. A spacecraft approaching the active field line where the emission is generated will detect the highest frequency emissions first, and progressively lower frequency emissions as it passes by the active field line. Thus, on a spectrogram, the resulting emission pattern appears "funnel-shaped". Further discussions of this effect can be found in Gurnett [1983] and references therein.

Terrestrial auroral hiss is commonly observed in association with strong field-aligned electron beams [Gurnett and Frank, 1972; Lin et al., 1984]. Specifically, in the nightside auroral zone, auroral hiss signals are correlated with intense inverted-V electron events having energies on the order of 10 keV [Gurnett and Frank, 1972]. In the polar cusp, auroral hiss is correlated with downward propagating field-aligned electron beams having energies of about 100 eV [Lin et al., 1984]. These electron beams are found at the low latitude edge of the polar cusp, on field-lines that are believed to map to the subsolar point of the magnetopause, where dayside reconnection occurs. Auroral hiss-like signals have even been generated by artificially created field-aligned electron beams ejected from the space shuttle, these beams having energies of about 1 keV [Gurnett et al., 1986; Farrell et al., 1988]. Clearly, there is a very strong association between auroral hiss signals and electron beams.

Modeling of the Jovian Auroral Hiss

As evident in Figure 3, for emissions propagating near the resonance cone, the group velocity vector is nearly perpendicular to the wave normal vector. Thus, the group velocity direction, ψ, can be quantified as $\mathrm{Tan}^2\psi \sim -\epsilon_{xx}/\epsilon_{zz}$. Using this expression, the evolution of a ray originating from a given source point can be determined. Such an analysis has been presented by Gurnett et al.,

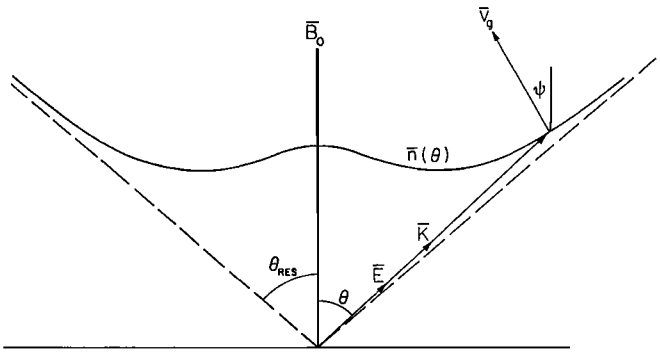

Fig 3. An illustration of the index of refraction surface showing the wave normal (k), electric field (E), and group velocity (v_g) geometry for wave propagation with wave normal angles, θ, near the resonance cone angle, θ_{res}.

[1983] and Lin et al., [1984] for terrestrial auroral hiss observed by the DE-1 spacecraft and by Morgan et al., [1990] for Jovian auroral hiss observed near the Io torus by the Voyager spacecraft. In these studies, the ray tracing was used to determine the location of the active field lines. Specifically, the source location and emitted rays were fit to match the occurrence of a single funnel-shaped auroral hiss emission observed on spectrograms. Here we present a similar two-dimensional analysis for the Jovian high-latitude auroral hiss observations.

In order to solve for the ray path, both the electron cyclotron frequency (i.e., magnetic field) and electron plasma frequency (i.e., electron density) at high latitudes are required. The observations of the auroral hiss are made beyond about 6 R_J, thus the internal components of the O4 magnetic field model [Connerney et al., 1981] are not necessary for accurate modeling of the field. However, the Jovian current sheet has a dramatic effect on the field lines, stretching them outward from a dipolar configuration. We have included the effects of this sheet in the ray tracing by incorporating the analytical expression presented in Connerney et al. [1981] for the magnetic field from the current, adding this to a dipole magnetic field model. Beyond about 3 R_J we obtain excellent agreement with the original O4 model.

Preliminary analysis of the solar wind plasma experiment data indicates that the plasma density decreases significantly with increasing latitude. Near the magnetic equator, the plasma-to-cyclotron frequency ratio, f_{pe}/f_{ce}, is well above unity. However, at latitudes above about 20°, this ratio drops well below unity. At the present time, a comprehensive plasma density model at high-latitudes based upon the Ulysses observations does not exist. However, to be consistent with the particle observations, we will set the ratio of f_{pe}/f_{ce} to a low value in order to model whistler-mode ray path behavior at high latitudes. Variations of this ratio will tend to change the shape of the auroral hiss funnel on a spectrogram, but will not affect the overall occurrence of the emission, which is dependent primarily upon the high latitude source position.

Figure 4 shows the results of the raytracing and corresponding fit (in the inset) for the event occurring between hour 1830 and 2400 on 7 February. To obtain the fit, the f_{pe}/f_{ce} ratio was set to a value of 0.14, consistent with the characteristic frequencies observed at this time (see Figure 1). In Figure 4, the rays represent the low latitude edge of the auroral hiss beam as a function of frequency. When the spacecraft is at latitudes above this edge, it is considered within the beam pattern. The inset panel shows the emission occurrence centered at hour 2200 on 7 February. The dotted line indicates the time when the spacecraft intercepted the modeled rays shown in the figure. The raytracing demonstrates that the funnel-shaped appearance of the emission results from the spacecraft flying through the low latitude edge of the emission beam originating from a high-latitude source, on field lines extending out to at least 65 R_J. This excursion into the beam reoccurs at the planetary rotation rate, as the magnetic pole tips toward the spacecraft, which explains the periodic reoccurrence of the emission approximately every 10 hours (as seen in Figure 1).

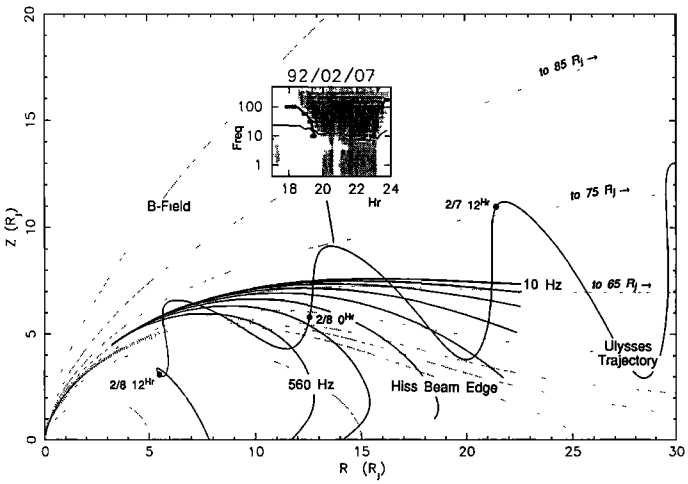

Fig 4. Results of ray tracing as applied to the auroral hiss emission observed centered at hour 2200 on 7 February 1992. The figure shows the low latitude edge of the auroral hiss beam at 10, 17, 31, 56, 100, 170, 310, and 560 Hz, respectively, whose source is on field lines extending out to 65 R_J. The inset shows the time and frequency of spacecraft interceptions with the modeled beam edge (indicated by dotted line), which is compared to the actual observations from the search coil and WFA receiver. Note that the initiation and cessation of the emission is consistent with a modeled source located on field lines at high latitudes.

The reoccurrence of the emission allows a fairly accurate determination of the active region. For example, if the source was located on field lines at lower latitudes than those shown in Figure 4, the emission would be observed for much longer times during each planetary rotation (i.e., the spacecraft would spend a longer time in the beam). In contrast, if the source was located on field lines at higher latitudes, the emission occurrence near closest approach, that occurring between hour 0400 and 0800 on 8 February, would not be observed. Thus, the reoccurrence of the emission during the inbound period localizes the set of active field lines associated with the emission source to the modeled region.

The model also suggests that auroral hiss is beamed upward from Jupiter (i.e., $\mathbf{k}\cdot\mathbf{B} > 0$ in the northern hemisphere). Repeated observations of the emission indicate that the funnel shape of the emission becomes less distinct as Ulysses approaches the planet. The raytracing analysis suggests that this effect is due to the reduced dispersion of the emission close to the planet (i.e., the rays are more tightly packed close to the low altitude edge of the source, as indicated in Figure 4). The opposite effect would be observed if the rays were beamed down the field line ($\mathbf{k}\cdot\mathbf{B} < 0$ in the northern magnetic hemisphere). The spin modulation signature of the E and B signals detected in the WFA further confirm the upward propagation of the emission. Specifically, the amplitude and wave phase of E and B as a function of spin phase are returned, and these measurements indicate that a signicant upward-directed Poynting flux component exists for this signal.

Since each of the whistler-mode funnels on a frequency-versus-time spectrogram appear complete (i.e., filled in with no emission "gaps" in the center of the pattern), we conclude the active region along the high-latitude magnetic field line is very extended, ranging from values < 5 R_J to at least 30 R_J. If the active region was of limited extent, then the funnel-shaped emission would have a distinct emission dropout in intensity in its central region [Farrell, 1990], making it appear more like a "saucer" emission [James, 1976]. Such an incomplete funnel pattern was not observed.

A high latitude source in the northern hemisphere can explain the occurrences of the auroral hiss emission during the inbound period. A similar conjugate source in the southern hemisphere can explain the first event observed during the outbound period (i.e., that between hour 0100 and 0500 on 9 February). However, at later times during the outbound period, the observations and model occurrences from the southern hemisphere conjugate location are no longer coincident, suggesting that either the plasma or magnetic field models used as the basis of the raytracing are no longer accurate or that the source has moved to a different set of L-shells (i.e., a temporal variation in source position).

The source location study presented above has some rather important consequences. Following the two Voyager flybys, it was believed that Io-related processes were the dominant (if not singular) energy source in the magnetosphere. Little, if any, evidence was presented for a solar wind/magnetosphere interaction. In the mid to late 1980s, evidence started to surface suggesting that a solar wind interaction is present. Specifically, the long-term behavior of at least two of the radio components was shown to be controlled externally by the solar wind [Desch and Barrow, 1984; Bolton et al., 1989]. However, the Ulysses observations of auroral hiss and the entry of solar wind-like particles occurring on field lines connected to the frontside magnetopause directly verify a solar wind energy source in the magnetosphere. Using these direct observations, the energy of the solar wind energy source can be quantified and compared to the Io energy source.

Power of the Jovian High Latitude Auroral Hiss

The radiated power of the high-latitude auroral hiss can be estimated by determining the Poynting flux through a cross-sectional area containing the whistler-mode rays. The Poynting vector is defined as

$$\mathbf{S} = \frac{1}{\mu_o}\mathbf{E} \times \mathbf{B} \qquad (1)$$

where $\mathbf{E}$ and $\mathbf{B}$ are the wave electric and magnetic field vectors, respectively. The frequency domain version of Ampere's law is

$$\mathbf{k} \times \mathbf{B} = \mu_o \epsilon \omega \mathbf{E} \ . \qquad (2)$$

Using $\mathbf{k} = \mathbf{n}\omega/c$ and $\epsilon = n^2 \epsilon_o$, where n is the wave index of refraction, and incorporating these into Eq. (2) yields

$$\mathbf{S} = -\frac{c}{\mu_o n}((\mathbf{n}\times\mathbf{B})\times\mathbf{B}) \ . \qquad (3)$$

From Gauss' magnetic law, $\mathbf{n}$ and $\mathbf{B}$ are perpendicular to each other, thus the Poynting flux becomes

$$S = \frac{cB^2}{\mu_o n} \qquad (4)$$

when considering the magnetic component of the wave. For whistler-mode emissions propagating near the resonance cone, the wave is quasi-electrostatic, and thus has an electric field consisting of a strong electrostatic component and weaker electromagnetic component. By definition, the wave magnetic field has only an electromagnetic component. It is the electromagnetic components of E and B that contribute to the Poynting flux and radiated power. In general, the Poynting flux expressions involving E tend to be complicated because a separation of the electromagnetic and electrostatic components must be made [Mosier and Gurnett, 1971; Farrell et al., 1988]. It is clearly much easier to use Eq. (4) above when magnetic measurements are available.

The auroral hiss magnetic component as measured by the Ulysses search coil can be used in Eq. (4) to determine the radiated power. In order to complete the calculation, the index of refraction must be known. The measured value of cB/E can be used to determine n, but care must be taken in the application (see Appendix). First, the measurements consist of wave components measured in the spin plane thus, at best, the ratio is an approximation to the real cB/E value. Second, only for parallel wave propagation (wave normal angle, θ, at 0°) does the measured cB/E ratio directly relate to the true index of refraction, cB/E ~ n. It is a common misconception that cB/E approximates n for oblique propagation. In fact, for propagation near the resonance cone ($\theta \sim \theta_{res}$), the cB/E ratio varies inversely with n (see Eq. (A-3)). Thus, near the resonance cone, as n approaches infinity, the measured cB/E ratio approaches zero, consistent with the measurement of a quasi-electrostatic wave.

Applying Eq. (A-3) to wave conditions measured near hour 1300 of 7 February (i.e., measured cB/E $\sim$ 1, $\epsilon_{zz} \sim -20$ and $\theta_{res} \sim 78°$ at 100 Hz), we find the value of the index of refraction to be about 5. The average magnetic field spectral density during this auroral hiss event is on the order of 10^{-7} nT^2/Hz, thus the Poynting flux is approximately $S = 6 \times 10^{-11}$ W/m^2. Presumably, the emission is emitted through an area subtending approximately 1/2 a hemisphere (i.e., 2π steradian) at 25 R_J which corresponds to 10^{19} m^2. This area is consistent with the raytracing results shown in Figure 4. Thus, the radiated power of this auroral hiss event is approximately 10^7 W.

Auroral hiss is commonly generated by auroral electron beams [Gurnett and Frank, 1972; Lin et al., 1984], which ultimately drive other auroral processes, such as discrete auroral arcs, etc. However, the beam-to-wave energy conversion efficiency is difficult to determine, since the efficiency depends on the beam energy. For a 1 keV electron beam, the whistler mode electromagnetic conversion efficiency was calculated to be about 10^{-4}–10^{-5} [Farrell et al., 1988], while the efficiency of faster moving beams modeled in simulations is on the order of 10^{-3} [Pritchett et al., 1989; Winglee and Kellogg, 1990]. These values suggest the auroral input power (i.e., energetic electron energy) driving the Jovian auroral hiss is on the order of 10^{10-12} W. We conclude that the auroral input power associated with the solar wind at Jupiter ($< 10^{12}$ W) is about 1% of the electrical driving power associated with Io (which is on the order of 10^{14} W [Hill et al., 1983]). The solar wind does contribute a considerable amount of energy, particularly when compared to the other magnetic planets. Yet, these energies are small when compared to Io-related electrical processes.

Appendix

Mosier and Gurnett [1971] derived the electric and magnetic wave amplitudes in a magnetoplasma assuming that the ambient magnetic field is aligned with the z-axis and the wave normal vector, **k**, lies in the x-z plane (see their Eq. (1)). During the inbound period, the Ulysses spin plane was quasi-perpendicular to the Jovian magnetic field. From Mosier and Gurnett [1971], the cB/E ratios for the wave components measured perpendicular to the ambient magnetic field is:

$$\frac{c\,b_y}{e_x} = n\cos\theta\left(\frac{\epsilon_{zz}}{\epsilon_{zz} - n^2\sin^2\theta}\right) \qquad \text{(A-1)}$$

where $\epsilon_{zz} = 1 - f^2_{pe}/f^2$ and θ is the wave normal angle. For wave propagation parallel to the ambient field (θ=0), Eq (A-1) reduces to

$$\frac{c\,b_y}{e_x} = n \qquad \text{(A-2)}$$

which suggests the measured cB/E ratio is a good indicator of the true wave index of refraction in this particular case. However, Eq. (A-2) is not accurate for oblique propagation. For example, for propagation near the resonance cone ($\theta \sim \theta_{res}$) the measured cB/E ratio becomes:

$$\frac{c\,b_y}{e_x} = -\frac{1}{n}\,\frac{\cos\theta_{res}}{\sin^2\theta_{res}}\,\epsilon_{zz} \qquad \text{(A-3)}$$

In this case, the measured cB/E ratio is inversely proportional to n. Thus, for emissions far out on the resonance cone, the measured cB/E ratios become small, representing the detection of a quasi-electrostatic wave.

References

Bame, S. J. et al., The Ulysses solar wind plasma experiment, *Astron. & Astrophys. Supp. Ser., 92*, 237, 1992a.

Bame, S. J., et al., Jupiter's magnetosphere: Plasma description from the Ulysses flyby, *Science, 257*, 1539, 1992b.

Bolton, S. J., S. Gulkis, M. J. Klein, I. dePater, and T. J. Thompson, Correlation studies between solar wind parameters and the decimetric radio emissions from Jupiter, *J. Geophys. Res., 94*, 121, 1989.

Connerney, J. E. P., M. H. Acuna, and N. F. Ness, Modeling the Jovian current sheet and inner magnetosphere, *J. Geophys. Res., 86*, 8370, 1981.

Desch, M. D., and C. H. Barrow, Direct evidence of solar wind control of Jupiter's hectometer wavelength radio emission, *J. Geophys. Res., 89*, 6819, 1984.

Farrell, W. M., D. A. Gurnett, P. M. Banks, R. I. Bush, and W. J. Raitt, An analysis of the whistler-mode radiation from the Spacelab-2 electron beam., *J. Geophys. Res., 93*, 153, 1988.

Farrell, W. M., Comment on "Pulsed electron beam emission in space" by Neubert et al., (1988), *J. Geomag. Geoelectr, 42*, 57, 1990.

Gurnett, D. A. and L. A. Frank, VLF hiss and related plasma observations in the polar magnetosphere, *J. Geophys. Res., 77*, 172, 1972.

Gurnett, D. A. and L. A. Frank, Plasma waves in the polar cusp: Observations from Hawkeye-1, *J. Geophys. Res., 83*, 1447, 1978.

Gurnett, D. A., S. D. Shawhan, and R. R. Shaw, Auroral hiss, Z-mode radiation and auroral kilometric radiation in the polar magnetosphere: DE-1 observations, *J. Geophys. Res., 88*, 329, 1983.

Gurnett, D. A., High latitude electromagnetic plasma wave emissions, in *High-latitude space plasma physics*, ed. B. Hultqvist and T. Hagsfor, Plenum Pub. Co., 1983.

Gurnett, D. A., W. S. Kurth, J. T. Steinberg, P. M. Banks, R. I. Bush, and W. J. Raitt, Whistler-mode radiation from the Spacelab-2 electron beam, *Geophys. Res. Lett., 13*, 225, 1986.

Hill, T. W., A. J. Dessler, and C. K. Goertz, Magnetospheric models, in *Physics of the Jovian magnetosphere* , ed. A. J. Dessler, Cambridge Univ. Press, 1983.

James, H. G., VLF saucers, *J. Geophys. Res., 81*, 501, 1976.

Lin, C. S., J. L. Burch, S. D. Shawhan, and D. A. Gurnett, Correlation of auroral hiss and upward electron beams near the polar cusp, *J. Geophys. Res., 89*, 925, 1984.

Morgan, D. D., D. A. Gurnett, W. S. Kurth, and F. Bagenal, The source position of Jovian "auroral" hiss (abstract), Magnetospheres of the Outer Planets Conference, Annapolis, MD, August, 1990.

Mosier, S. R. and D. A. Gurnett, Theory for the Injun 5 very low frequency Poynting flux measurements, *J. Geophys. Res., 76*, 972, 1971.

Pritchett, P. L., H. Karimabadi, and N. Omidi, Generation mechanism of whistler waves produced by electron beam injection in space, *Geophys. Res. Lett., 16*, 883, 1989.

Simpson, J. A., et al., Energetic charged particle phenomena in the Jovian magnetosphere: First results from the Ulysses COSPIN collaboration, *Science, 257*, 1543, 1992.

Stone, R. G., et al., The ISPM unified radio and plasma wave experiment, ESA Special Publication, SP-1050, 1983.

Stone, R. G., et al., The unified radio and plasma wave investigation, *Astron. & Astrophys. Supp. Ser., 92*, 291, 1992a.

Stone, R. G. et al., Ulysses radio and plasma wave observations in the Jupiter environment, *Science, 257*, 1524, 1992b.

Winglee, R. L., and P. J. Kellogg, Electron beam injection during active experiments: 1. Electromagnetic wave emissions, *J. Geophys. Res., 95*, 6167, 1990.

W. M. Farrell, R. J. MacDowall, M. D. Desch, M. L. Kaiser and R. G. Stone, Laboratory for Extraterrestrial Physics, NASA/Goddard Space Flight Center, Greenbelt MD 20771

P. J. Kellogg and N. Lin, Univ. of Minnesota, School of Astronomy & Astrophysics, Minneapolis MN 55455

N. Comilleau-Wehrlin, and P. Canu, Centre de Recherches en Physique de l'Environnement Terrestre et Planetaire (CRPE), 92131 Issy-les-Moulineaux, France

S. J. Bame and J. L. Phillips, Space Plasma Physics Group, Los Alamos National Laboratory, Los Alamos NM 87545

(Received February 5, 1993;
accepted April 7, 1993.)